Available online at www.sciencedirect.com
ScienceDirect
Journal of Solid State Chemistry 180 (2007) 1381–1389
JOURNAL OF SOLID STATE CHEMISTRY
www.elsevier.com/locate/jssc

# Two non-centrosymmetric cubic seleno-germanates related to CsCl-type structure: Synthesis, structure, magnetic and optical properties

Amitava Choudhury, Larisa A. Polyakova, Sabine Strobel, Peter K. Dorhout*

*Department of Chemistry, Colorado State University, Fort Collins, CO 80523, USA*

Received 15 September 2006; received in revised form 1 February 2007; accepted 4 February 2007
Available online 17 February 2007

**Abstract**

Two related non-centrosymmetric, cubic, quaternary chalcogenides, containing europium have been synthesized employing the molten flux method and by the reaction of europium halides with the ternary seleno-germanate, $Na_6Ge_2Se_6$. The reactions of Eu, Ge and Se were accomplished in a molten $Na_2Se_2$ flux at 800 °C for 150 h in an evacuated fused silica ampoule and yielded $Na_2EuGeSe_4$ (**I**). Similarly, $Na_{0.75}Eu_{1.625}GeSe_4$ (**II**), could be synthesized at slightly lower temperature (750 °C) with a different starting ratio of Eu, Ge, Se and $Na_2Se_2$. A reaction between $EuCl_3$ and $Na_6Ge_2Se_6$ in 1:2 ratio at 650 °C for 96 h in an evacuated fused silica ampoule yielded $Na_2EuGeSe_4$ (**I**), while the reaction between $EuI_2$ and $Na_6Ge_2Se_6$ in 1:1 ratio under similar conditions yielded $Na_{0.75}Eu_{1.625}GeSe_4$ (**II**). Crystal data for these compounds are as follows: **I**, cubic, space group $I\bar{4}3m$ (no. 217), $a = 7.3466(3)$, $Z = 2$; **II**, cubic, space group $I\bar{4}3d$ (no. 220), $a = 14.7065(8)$, $Z = 16$. The crystal structures of **I** and **II** are closely related and can be compared to a CsCl-type and its ordered superstructure, respectively. These compounds are semiconductors with optical band gaps around 2 eV. The temperature dependence of the magnetic susceptibility indicated that both compounds are paramagnetic with $\mu_{\text{eff.}} = 7.6$ and $7.73\,\mu_B$, for **I** and **II**, respectively, close to the theoretical value of $7.94\,\mu_B$ for $Eu^{2+}$. Raman spectroscopic characterization of the compounds is also reported.


*Keywords:* Chalcogenide; Europium; Semiconducting; CsCl type; Superstructure

## 1. Introduction

The synthesis, structure and studies of quaternary compounds involving an alkali cation, rare earth, main group element and a chalcogen atom are especially attractive because they comprise a large number of materials, through the permutation and combination of the elements [1]. This family of compounds also exhibits interesting properties, for example, luminescence [2] and ferroelectricity [3]. Molten alkali polychalcogenide flux or alkali halide flux synthesis techniques are often employed in the exploration of such families of solids [4,5]. In the molten chalcogenide flux, the main group element often reacts to form a well-defined building unit, which becomes the anionic building block of the quaternary compound. For a particular building unit, the variation of the trivalent lanthanide cations often has little impact on the crystal structures. Thus, a series of compounds could be synthesized by varying the lanthanide cations for example $CsLnSiS_4$ ($Ln$ = Sm–Tm) [6]. A similar variation of alkali metal cations, keeping the anionic moiety and lanthanide ion fixed, is not always feasible and leads to altogether new crystal structures. This is especially true when moving from the heavier to the lighter alkali metals like Na and Li due to the smaller cationic radius and lower basicity, they tend to form different structures. For example, isostructural $ASmGeSe_4$ ($A$ = K, Rb, Cs) can be made except the Na-analogue [7], the existence of which was recently realized in the form of a salt-inclusion compound, $NaSmGeSe_4 \cdot 0.25Na_2Se$ [8]. Broadly speaking, a series of isostructural compounds is known with the general formula $ALnTtQ_4$ ($A$ = K, Rb, Cs; $Ln$ = Lanthanide element, $Tt$ = Ge, Si and $Q$ = S or Se), but none so far with Na and Li cations [6,7,9–17]. For this reason, our group has been trying to incorporate Na cations in the rare earth main group chalcogenide matrix to prepare new structures by employing various synthetic routes, including

*Corresponding author. Fax: +1 970 491 1801.
*E-mail address:* pkd@lamar.colostate.edu (P.K. Dorhout).

0022-4596/$ - see front matter © 2007 Elsevier Inc. All rights reserved.
doi:10.1016/j.jssc.2007.02.002

the chalcogenide flux synthesis [18]. Towards this goal, we have synthesized two new $Na^+$-containing non-centrosymmetric cubic quaternary compounds, $Na_2EuGeSe_4$ (**I**) and $Na_{0.75}Eu_{1.625}GeSe_4$ (**II**). In this paper, we present the synthesis, structure, and some physical properties of these two compounds and also discuss them as disordered CsCl-type structure (**I**) and its ordered superstructure (**II**). We have also attempted to compare and contrast the structures of **I** and **II** with analogous structures reported in the literature [19–28].

## 2. Experimental section

### 2.1. Syntheses

Compounds **I** and **II** were prepared by the well-known reactive flux method using the alkali metal binary polychalcogenides as well as by the reaction of metal halide with ternary sodium seleno-germanate. The following reagents were used as received and stored in an inert atmosphere glovebox: europium (Eu: 99.95%, Ames Laboratory), germanium (Ge: 99.999%, Cerac), selenium (Se: 99.999%, Johnson-Mathey), $EuCl_3$ and $EuI_2$ (99.9%, Aldrich). $Na_2Se_2$ and $Na_6Ge_2Se_6$ were made from a stoichiometric combination of the elements in liquid ammonia and in a sealed ampoule, respectively, as previously described [29,30]. The reactants were directly loaded into fused silica ampoules inside an $N_2$-filled atmosphere glovebox; whereas for metal halide and ternary seleno-germanate reactions, the reactants were first thoroughly ground in an agate mortar and then transferred to a graphite crucible, which was then placed inside the fused silica ampoule. The ampoules were flame-sealed under vacuum and placed in a temperature-controlled furnace.

### 2.2. Flux route

$Na_2EuGeSe_4$, **I**, was synthesized by combining 43.4 mg of Eu (0.285 mmol), 52.1 mg of Ge (0.717 mmol), 62.4 mg of Se (0.79 mmol), and 116.8 mg of $Na_2Se_2$ (0.573 mmol) with an approximate compositional ratio of 8Na:2Eu:5Ge:13.5Se. The furnace was ramped to 800 °C at a rate of 35 °C/h and held constant at 800 °C for 150 h and then slowly cooled (4 °C/h) to room temperature. After the product cooled, the ampoules were opened in an inert atmosphere glovebox, and the solid product was soaked in *N*,*N*-dimethylformamide (DMF) for 6 h in order to dissolve and wash away any remaining flux and loosen the product crystals. The majority of the product contained red crystals along with few yellowish crystals and some colorless plates. The unit cell parameters collected on the crystalline products indicated that the red crystals comprised a new material and subsequent full data set analysis revealed the formula to be $Na_2EuGeSe_4$, while the yellow and colorless plates turned out to be $Na_2GeSe_3$ and $GeSe_2$, respectively [31,32].

$Na_{0.75}Eu_{1.625}GeSe_4$, **II**, was synthesized by combining 39.6 mg of Eu (0.260 mmol), 47.6 mg of Ge (0.655 mmol), 77.4 mg of Se (0.98 mmol), and 53.5 mg of $Na_2Se_2$ (0.262 mmol) with an approximate compositional ratio of 4Na:2Eu:5Ge:11.5Se. The furnace was ramped to 750 °C at a rate of 35 °C/h and held constant at 750 °C for 150 h and then slowly cooled (4 °C/h) to room temperature. After DMF treatment, orange-red crystals were chosen for the single-crystal analysis. The product also contained some uncharacterized yellowish powder as a minor component.

### 2.3. Metal halide route

$Na_2EuGeSe_4$, **I**, was synthesized by combining 25.8 mg of $EuCl_3$ (0.1 mmol) and 151.4 mg of $Na_6Ge_2Se_6$ (0.2 mmol) with an exact compositional ratio of $Na_6Ge_2Se_6$:2$EuCl_3$. The furnace was ramped to 650 °C at a rate of 35 °C/h and held constant at 650 °C for 96 h and then slowly cooled (5 °C/h) to room temperature. The product, after treatment with DMF, revealed red cubes of $Na_2EuGeSe_4$, orange-red plates of $Na_8Eu_2(Ge_2Se_6)$ [18], and yellow crystals of $Na_2GeSe_3$. EDS analysis performed on individual hand-picked red cubic crystals indicated the presence of Na, Eu, Ge, and Se and gave an approximate composition of $Na_{1.88}Eu_{0.94}GeSe_{3.78}$. The identities of the compounds were established by the unit cell parameters collected on several single crystals. A few milligrams of the very distinct red-cubic shaped crystals were manually picked up under the microscope for magnetic study.

$Na_{0.75}Eu_{1.625}GeSe_4$, **II**, was synthesized by combining 40.6 mg of $EuI_2$ (0.1 mmol) and 75.7 mg of $Na_6Ge_2Se_6$ (0.1 mmol) with an exact compositional ratio of $Na_6Ge_2Se_6$: $EuI_2 = 1{:}1$. The furnace was ramped to 650 °C at a rate of 35 °C/h and held constant at 650 °C for 96 h and then slowly cooled (5 °C/h) to room temperature. The product, after treatment with DMF, revealed the presence of red cubic crystals and some unidentified yellow poly-crystals. A single-crystal X-ray data set was collected on the red crystal to establish the composition of Na/Eu in the structure and found exactly same as obtained from the alkali selenide flux method, $Na_{0.75}Eu_{1.625}GeSe_4$. EDS analysis performed on individual red crystals indicated the presence of Na, Eu, Ge, and Se and gave an approximate composition of $Na_{0.48}Eu_{1.67}GeSe_{3.8}$. A few milligrams of red cubes were picked from this batch of sample for the magnetic study.

### 2.4. X-ray structure determination

X-ray diffraction data sets of single crystals were collected on a Bruker Smart CCD diffractometer. These data were integrated with SAINT [33], the program HABITUS was used for numerical absorption correction [34]. The structures were solved by direct methods using SHELXS-97 [35] and refined using SHELXL-97 [36]. The last cycles of refinement included an anisotropic thermal parameter refinement for all the atoms in the case of **I** and

for the non-disordered atoms of **II**. The space group for compound **I** was unambiguously assigned to $I\bar{4}3m$ (no. 217) based on the systematic absences and better combined figure of merit compared to $Im\bar{4}m$ and $I23$. The position of Ge, Se and Eu were easily assigned from the difference Fourier maps; however, the isotropic refinement indicated high thermal parameters for Eu and the highest difference between the peak (12.32) and deepest hole (−21.45) were high with the absence of any significant *q*-peaks; the *R*-factor ($wR_2 = 62.94\%$) did not converge to the expected value (~10%). This led us to believe that there may be a disorder in the Eu site due the mixed occupancy of Na and Eu. So in the next cycle of refinement, this site was refined by putting both Na and Eu, keeping their coordinates same while freely refining their occupancies, constraining the sum of the occupancy of Na and Eu to be 100%. Such refinement yielded a satisfactory *R*-factor ($wR_2 = 11\%$), thermal parameters for Eu and Na and gave occupancies of 32% and 68%, respectively, for Eu and Na, which were then fixed to 33.333% and 66.667% (Eu: 1/3 and Na: 2/3), respectively, to get a charge-balanced formula. The Flack parameter converged to a value of 0.1(3) and a racemic twin refinement was performed. The twin refinement did not improve the *R*-factor and gave a BASF value same as that of Flack parameter. There was only one choice of space group ($I\bar{4}3d$, no. 220) for compound **II**, based on the systematic absences. The four atoms, one Eu, two Se one Ge were immediately assigned from the difference Fourier maps and refined isotropically with very good thermal parameters. There were several *q*-peaks with low electron density (9.5–3 $e^-$/site) and the strongest one appearing close to Eu. So anisotropic refinement was then carried out, which indicated three low intensity *q*-peaks (7.65, 6.10 and 3.83 $e^-$/site) to be assigned. These peaks are quite close (0.7–0.9 Å) to each other, indicating the possibility of a disorder. These peaks were initially assigned as Na atoms and their occupancies refined freely, but the peak with 7.66 $e^-$/site exhibited high thermal parameter ($U_{11} = 0.11$) with an occupancy of 80% (on a two-fold symmetry, Wyckoff = 24*d*), which is more than necessary to balance the remaining positive charge, while two other Na-atoms refined well with 41% and 30% occupancies in four-fold and two-fold symmetry positions, respectively. The 7.66 $e^-$/site peak was assigned as Eu, taking hints from previously solved similar structures [24,26]. Eu refines well with an occupancy of 8.5% and a satisfactory thermal parameter was obtained. In order to obtain a charge-balanced formula, the occupancies of Eu (Eu2, Wyckoff = 24*d*) and the two Na-sites (Na1A, Wyckoff = 12*a* and Na1, Wyckoff = 24*d*) were made 8.33%, 40%, and 30%, respectively, and then subsequently refined. The close contacts between the disordered atoms (Eu2, Na1 and Na1A) can be safely ignored because their occupancies were less than 50%. However, refinement of the Flack parameter did not converge to 0 [0.8(2)] indicating an incorrect absolute structure, so it was inverted for final refinement, which yielded a Flack parameter of 0.12. A racemic twin refinement was performed, which did not improve the *R*-factor and gave a BASF value same as that of Flack parameter. The non-convergence of the Flack parameter to 0 in both the compounds indicates that not all $GeSe_4$ tetrahedra are pointing in one direction, in other words there is small fraction of the other enantiomer present in the single crystal. Details of the final refinements and the cell parameters for **I** and **II** are given in Table 1. The final atomic coordinates and the isotropic displacement parameters for **I** and **II** are given in Table 2. Selected inter-atomic distances are listed in Table 3. It should be noted that both the structures can be solved in lower symmetry tetragonal system in the space groups $I\bar{4}$ and $I\bar{4}2d$, respectively, for **I** and **II**, however, the disorder issues remained the same in the two structures. So we preferred to solve the structures in cubic system. Further details of the crystal structure investigations can be obtained from the Fachinformationszentrum Karlsruhe, 76344 Eggenstein-Leopoldshafen, Germany, (fax: +49 7247 808 666; e-mail: crysdata@fiz.karlsruhe.de) on quoting the depository number CSD-416885 ($Na_{0.75}Eu_{1.625}GeSe_4$) and CSD-416886 ($Na_2EuGeSe_4$).

### 2.5. Physical property measurements

The bulk solid-state Raman spectra were collected on a Nicolet Magna-IR 760 spectrometer with a FT-Raman Module attachment by use of a Nd:YAG excitation laser (1064 nm). Diffuse reflectance measurement for the compounds were done on a Varian Cary 500 UV–vis–NIR spectrophotometer equipped with a Praying Mantis accessory. A polyTeflon standard was used as a reference. The Kubelka–Munk function was applied to obtain band gap information [37]. Magnetic susceptibilities of **I** and **II** were measured at 0.5 T over the temperature range 1.8–300 K and isothermal magnetization at 1.8 K up to a field of 5 T was measured with a Quantum Design SQUID magnetometer.

## 3. Results and discussion

### 3.1. Structure description

Compound **I** crystallizes in the non-centrosymmetric space group of $I\bar{4}3m$ and is isostructural to the previously reported compounds; $Tl_3MQ_4$ ($M$ = V, Nb, Ta; $Q$ = S, Se) [19], $Na_3SbQ_4$ ($Q$ = S, Se) [20,21], and $K_2BaSnTe_4$ [22]. The asymmetric unit of **I** contains atoms in three crystallographic sites occupied by Ge, Se and constitutionally disordered Na and Eu. Close inspection of the structure reveals that it can be related to a CsCl-type structure. If a cubic unit cell is imagined to be divided into eight smaller cubes, and each of the eight cubes have cations at all corners and anions occupy the center of four of these smaller cubes, then an antifluorite lattice is formed [38]. In compound **I**, the origin is already at a cation site and Ge atoms are located at the eight corners and the body center

Table 1
Crystal data and structural refinement parameters for compounds **I** and **II**

| Compounds | **I** | **II** |
|---|---|---|
| Empirical formula | $Na_2EuGeSe_4$ | $Na_{0.75}Eu_{1.625}GeSe_4$ |
| Formula weight | 586.37 | 652.61 |
| Crystal system | Cubic | Cubic |
| Space group | $I\bar{4}3m$ | $I\bar{4}3d$ |
| $a$ (Å) | 7.3466 (3) | 14.7065(8) |
| Volume (Å$^3$) | 396.51(3) | 3180.7(3) |
| $Z$ | 2 | 16 |
| $\rho_{calc}$ (g cm$^{-3}$) | 4.911 | 5.451 |
| $T/K$ | 293(2) | 293(2) |
| $\theta$ range (°) | 3.92–25.98 | 3.39–25.35 |
| Index ranges | $-8 \leqslant h, k, l \leqslant 8$ | $-17 \leqslant h, k, l \leqslant 17$ |
| $\mu$ (mm$^{-1}$) | 29.987 | 34.675 |
| $F(000)$ | 506 | 4458 |
| Total data collected | 1593 | 11628 |
| Unique data | 86 | 498 |
| Observed data ($\sigma > 2\sigma$ ($I$)) | 83 | 465 |
| Refinement method | Full-matrix least-squares on $\lvert F^2\rvert$ | Full-matrix least-squares on $\lvert F^2\rvert$ |
| $R$ indices [$I > 2\sigma(I)$] | $R_1 = 0.0458$[a], w$R_2 = 0.0985$[b] | $R_1 = 0.0326$[a], w$R_2 = 0.0832$[b] |
| $R$ indices (all data) | $R_1 = 0.0463$, w$R_2 = 0.0983$ | $R_1 = 0.0360$, w$R_2 = 0.0848$ |
| Goodness of fit ($S$) | 1.201 | 1.139 |
| No of variables | 8 | 29 |
| Largest difference map peak and hole (eÅ$^{-3}$) | 1.177 and −1.036 | 0.927 and −1.140 |

[a] $R_1 = \Sigma||F_o|-|F_c||/\Sigma|F_o|$.
[b] $wR_2 = \{\Sigma[w(F_o^2-F_c^2)^2]/\Sigma[w(F_o^2)^2]\}^{1/2}$, $w = 1/[\sigma^2(F_o)^2 + (aP)^2 + bP]$ where $P = [F_o^2 + 2F_c^2]/3$; $a = 0.0167$ and $b = 28.2368$ for **I**; $a = 0.0348$ and $b = 89.3287$ for **II**.

Table 2
Atomic coordinates ($\times 10^4$) and equivalent isotropic displacement parameters (Å$^2 \times 10^3$) for compounds **I** and **II**

| Atoms | Wyckoff | $x$ | $y$ | $z$ | $U_{eq}$ | Occupancy |
|---|---|---|---|---|---|---|
| I | | | | | | |
| Ge(1) | 2*a* | 0 | 0 | 0 | 21(1) | 100 |
| Se(1) | 8*c* | 1851(2) | 1851(3) | 1851(3) | 39(1) | 100 |
| Eu(1) | 6*b* | 0 | 5000 | 0 | 42(1) | 33.33 |
| Na(1) | 6*b* | 0 | 5000 | 0 | 42(1) | 66.67 |
| II | | | | | | |
| Ge(1) | 16*c* | 2586(1) | 2414(1) | 7586(1) | 18(1) | 100 |
| Eu(1) | 24*d* | 5000 | 2500 | 9823(1) | 51(1) | 100 |
| Se(1) | 16*c* | 3505(1) | 1495(1) | 8505(1) | 34(1) | 100 |
| Se(2) | 48*e* | 4022(1) | 4226(1) | 9063(1) | 33(1) | 100 |
| Eu(2) | 24*d* | 239(1) | 0 | 7500 | 58(4) | 8.33 |
| Na(1A) | 12*a* | 1250 | 0 | 7500 | 28(5) | 40 |
| Na(1) | 24*d* | 180(2) | 0 | 7500 | 40(6) | 30 |

[a] $U_{eq}$ is defined as one-third of the trace of the orthogonalized $U_{ij}$ tensor.

of the cubic unit cell, Na/Eu occupy the edge center and face center while the Se atoms are located inside all eight smaller cubes (Fig. 1). So **I** may be viewed as a filled anti-fluorite-type structure, or more appropriately a CsCl-type structure, because each smaller cube has cations at all eight corners and anion at the center. There is a big difference in size and coordination preference between the Ge and Eu/Na atoms. For example, each Na/Eu is surrounded by four Se atoms in an elongated tetrahedral coordination with short Eu/Na–Se distances of 3.008(2) Å, while there are four more Se atoms around it in a compressed tetrahedral coordination with slightly longer Eu/Na–Se distances of 3.543(2) Å. The overall eight-fold coordinating polyhedron is called trigonal dodecahedron (Fig. 2). However, Ge is surrounded by four Se in a perfect tetrahedral coordination with Ge–Se distances of 2.355(3) Å and Ge–Se–Ge bond angles of 109.5(1)°. Selenium, on the other hand, does not have a symmetric eight-fold coordination, rather Se has

Table 3
Selected inter atomic distances for compounds **I** and **II**

| | | | |
|---|---|---|---|
| I | | | |
| Ge(1)–Se(1) | 2.355(3) | Eu(1)/Na(1)−Se(1) × 4 | 3.0084(3) |
| Ge(1)–Se(1)$^{\#1}$ | 2.355(3) | Eu(1)/Na(1)−Se(1) × 4 | 3.5433(5) |
| Ge(1)–Se(1)$^{\#2}$ | 2.355(3) | | |
| Ge(1)–Se(1)$^{\#3}$ | 2.355(3) | | |
| II | | | |
| Ge(1)–Se(1) | 2.341(3) | Na(1A)−Se(2)$^{\#17}$ | 2.720(1) |
| Ge(1)–Se(2)$^{\#1}$ | 2.362(1) | Na(1A)−Se(2)$^{\#20}$ | 2.720(1) |
| Ge(1)–Se(2)$^{\#2}$ | 2.362(1) | Na(1A)−Se(2)$^{\#1}$ | 2.720(1) |
| Ge(1)–Se(2)$^{\#3}$ | 2.362(1) | Na(1A)−Se(2)$^{\#19}$ | 2.720(1) |
| | | Na(1)−Se(2)$^{\#17}$ | 2.631(2) |
| Eu(1)–Se(2)$^{\#\#6}$ | 3.076(1) | Na(1)−Se(2)$^{\#1}$ | 2.631(2) |
| Eu(1)–Se(2)$^{\#7}$ | 3.076(1) | Na(1)−Se(2)$^{\#19}$ | 3.032(2) |
| Eu(1)–Se(2)$^{\#8}$ | 3.124(1) | Na(1)−Se(2)$^{\#20}$ | 3.032(2) |
| Eu(1)–Se(2) | 3.124 (1) | Eu(2)−Se(2)$^{\#17}$ | 2.806(7) |
| Eu(1)–Se(1) | 3.283(1) | Eu(2)−Se(2)$^{\#1}$ | 2.806(7) |
| Eu(1)–Se(1)$^{\#8}$ | 3.283(1) | Eu(2)−Se(1)$^{\#18}$ | 3.113(7) |
| Eu(1)–Se(2)$^{\#9}$ | 3.581(1) | Eu(2)−Se(2)$^{\#19}$ | 3.547(6) |
| Eu(1)–Se(2)$^{\#10}$ | 3.581(1) | Eu(2)−Se(2)$^{\#20}$ | 3.547(6) |

Symmetry transformations used to generate equivalent atoms: For compound **I**; #1 $x, -y, -z$; #2 $-x, y, -z$; #3 $-x, -y, z$. For compound **II** #1 $y-1/4, x-1/4, z-1/4$; #2$-x+3/4, -z+5/4, y+1/4$; #3$z-3/4, -y+3/4, -x+5/4$; #6$-y+1, z-1/2, -x+3/2$; #7 $y+0, -z+1, -x+3/2$; #8$-x+1, -y+1/2, z+0$; #9 $z-1/4, y-1/4, x+3/4$; #10 $-z+5/4, -y+3/4, x+3/4$; #17 $y-1/4, -x+1/4, -z+7/4$; #18 $x+0, -y+0, -z+3/2$; #19 $-y+1/2, z-1, -x+1$; #20 $-y+1/2, -z+1, x+1/2$.

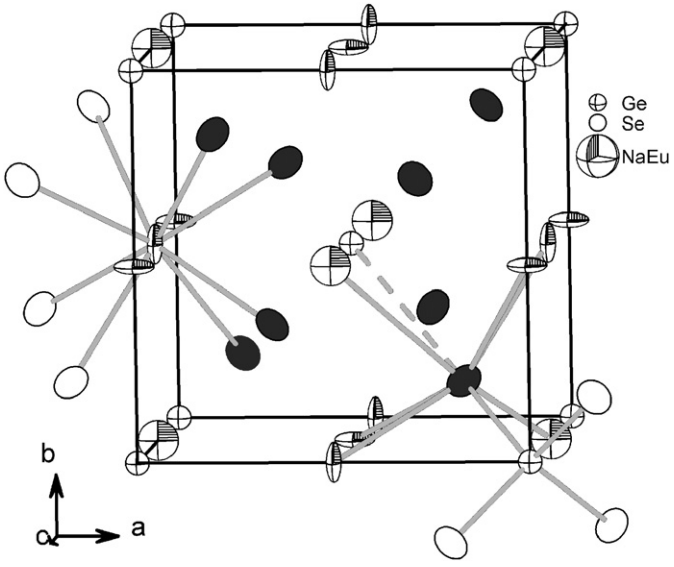


Fig. 1. The packing of atoms in one unit cell of **I**. The ball and stick representation of the different atoms in their polyhedral environments are also shown. Filled grey circles represent Se atoms inside the unit cell, while the dashed line is intended to indicate the eighth coordination of the Se anion. The thermal ellipsoids are given at 50% probability.

seven-fold coordination with three short and three long Se–Eu/Na bonds and one Se–Ge bond. The non-centrosymmetric nature of the structure arises from the arrangement of the $GeSe_4$ tetrahedra, all of which are pointing in the same direction responsible for the absence of a center of inversion as can be seen in Fig. 3.

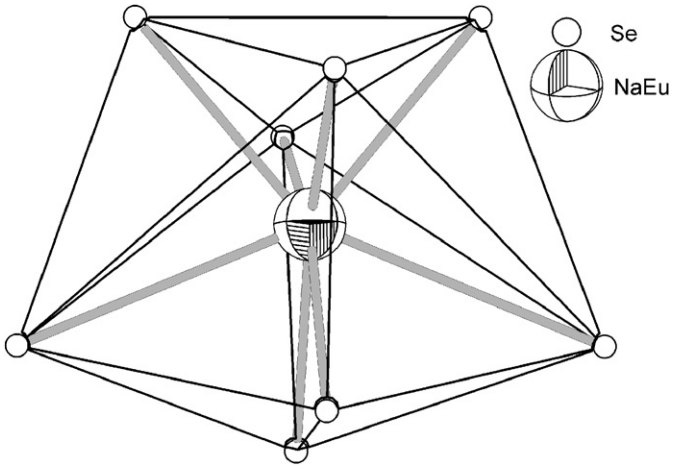


Fig. 2. The trigonal dodecahedron environment of Na/Eu site in **I**.

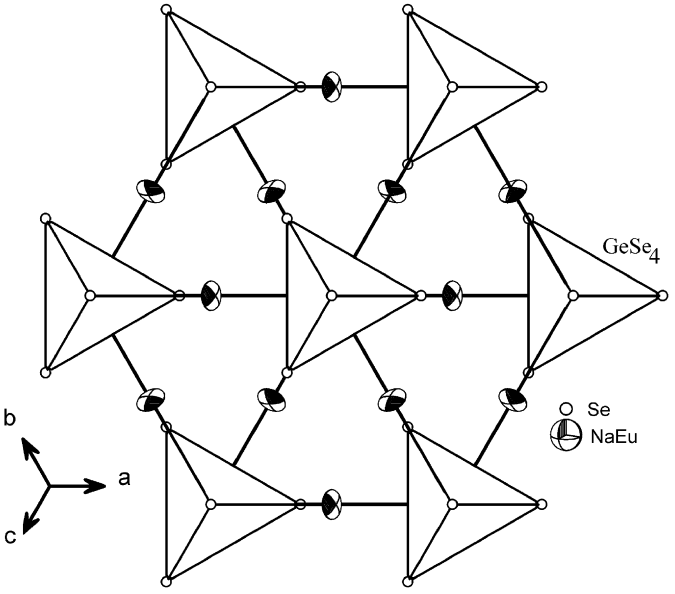


Fig. 3. The structures of **I** viewed along the [111] direction showing all the $GeSe_4$ tetrahedra pointing in same direction, indicating the non-centrosymmetric nature of the structure.

Compound **II**, crystallizes in the cubic non-centrosymmetric space group $I\bar{4}3d$ (no. 220) and is best described as an ordered super structure of **I. II**, is related to a series of cubic compounds for example, $Ba_3CdSn_2S_8$, $Ba_6Ag_2CdSn_4S_{16}$ [23], $Na_{1.5}Pb_{0.75}PSe_4$, $A_{0.5}Pb_{1.75}GeQ_4$ ($A$ = Na, Ag; $Q$ = S, Se), $Li_{0.5}Pb_{1.75}GeS_4$, $Ag_{0.5}Eu_{1.75}GeS_4$, $PbGeS_4$ [24–26] and $M_{0.5}Pb_{1.75}SiSe_4$ ($M$ = Cu and Ag) [27]. In **I**, Eu and Na are statistically disordered on the 6*b* site with 33.33% Eu and 66.67% Na. In **II**, more Na is substituted in the Eu site, which leads to an ordering of Eu, and the Eu and Na sites split into two distinct crystallographic sites with the doubling of the cell parameters in all directions; thus, a superstructure is derived (Fig. 4). If the Eu and the

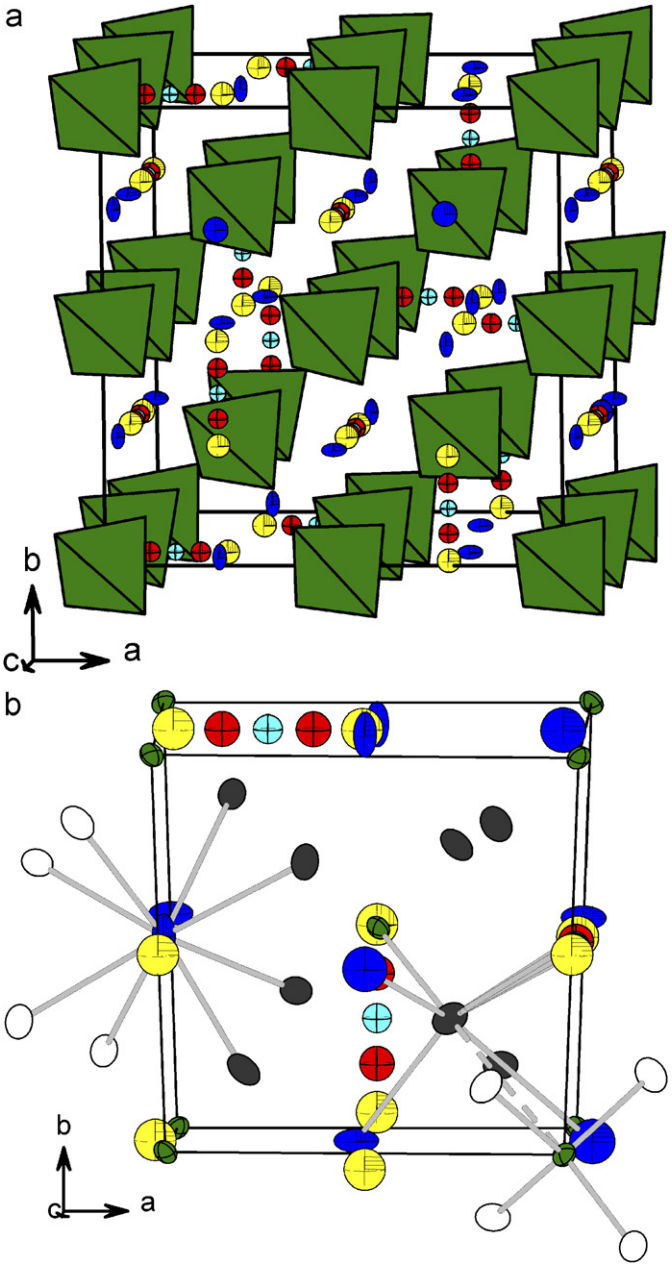


Fig. 4. (a) The packing of atoms in the superstructure cell of **II** (the color code for the circles is as follows: blue—Eu1, yellow—Eu2, red—Na1, and cyan—Na1A. (b) 1/8th of the unit cell of **II** (color code of the circles as above). Filled grey circles represent Se atoms inside the unit cell, while the dashed line is intended to indicate the eighth coordination of the Se anion. The thermal ellipsoids are given at 50% probability.

Na sites are labeled "*A*" and "*B*"-sites, respectively, then the *B*-site also has a minor Eu content in it along with Na. The asymmetric unit of **II** contains two crystallographically independent Se, one Ge and one Eu (Eu1) atom and disordered Na (Na1 and Na1A) and Eu (Eu2) atom sites. The cubic unit cell of **II** can be imagined to be divided into eight smaller cubes and each of these cubes can be considered to be equivalent to the unit cell of **I** (Fig. 4b). Ge is located at the eight corners and the body center of the smaller cubes. Eu1 and Eu2 occupy the edge- and the face center of each of the smaller cubes, while Se1 and Se2 occupy the eight eight-coordinated sites of each of the smaller cubes (two sites by Se1 and six sites by Se2). Na1 and Na1A are located in between Eu2 atoms. Ge is surrounded by four Se atoms in a nearly perfect tetrahedral coordination with Ge–Se distances in the range 2.341(3)–2.362(1) Å and Se–Ge–Se angles in the range 108.06(6)–110.84(5)°. Eu1 is in trigonal dodecahedron coordination as in **I** with Eu1–Se distances in the range 3.076(2)–3.580(1) Å. Cation site *B* is disordered between Na1/Na1A and Eu2, equivalent atom of Na1 is generated at 1.619(2) Å away from itself by applying symmetry. There are eight Se atoms surrounding the disordered Na1/Na1A/Eu2 site with the Na1/1A–Se and Eu2–Se distances in the range 2.631(2)–3.648(3) Å and 2.805(2)–3.547(3) Å, respectively. Similar to compound **I**, the non-centrosymmetric nature of the structure of **II** arises from the arrangement of $GeSe_4$ tetrahedra, which are all pointing in one direction (Fig. 5).

It is probably useful to compare the structure of **II** with similar known structures in the Na–Pb–Ge–Se/S system [24,26]. In these related structures, a higher degree of Pb substitution is found on the *B*-site than that of Eu in **II**. Apart from this difference in the composition, they are identical in all respects from a structural point of view. However, they are discussed for the first time as the *A*-site ordered superstructure of $Na_2EuGeSe_4$, **I**, which can be related to a CsCl-type structure. Though related Li-analogues of **I** are known, namely $Li_2PbGeS_4$ and $Li_2EuGeS_4$, they crystallize in lower symmetry tetragonal crystal system with a slightly different structure type [28]. To our knowledge, the CsCl-type structure and its ordered superstructure have not been reported in the quaternary

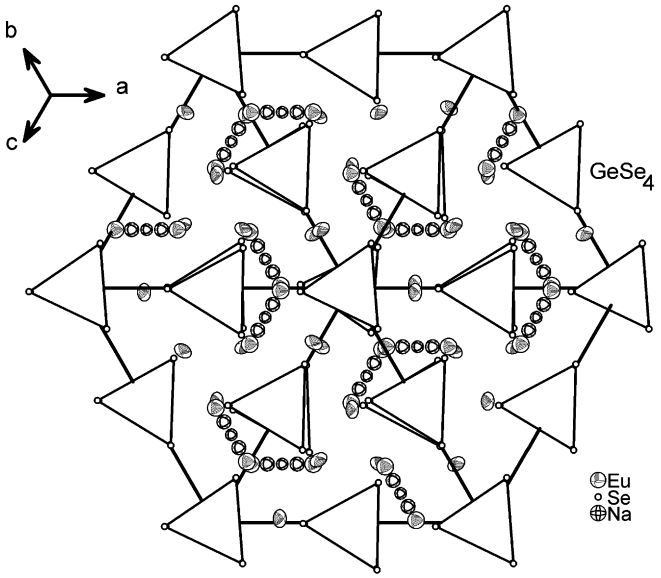


Fig. 5. The structures of **II** viewed along the [111] direction showing all the $GeSe_4$ tetrahedra pointing in same direction, indicating the non-centrosymmetric nature of the structure.

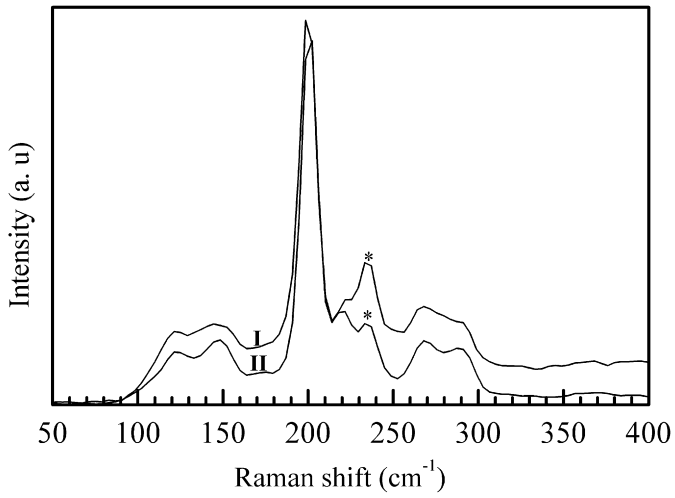


Fig. 6. Raman spectra for compounds **I** and **II**. The peaks indicated by an asterisk are due to elemental Se, produced by the decomposition of the compounds during the laser heating.

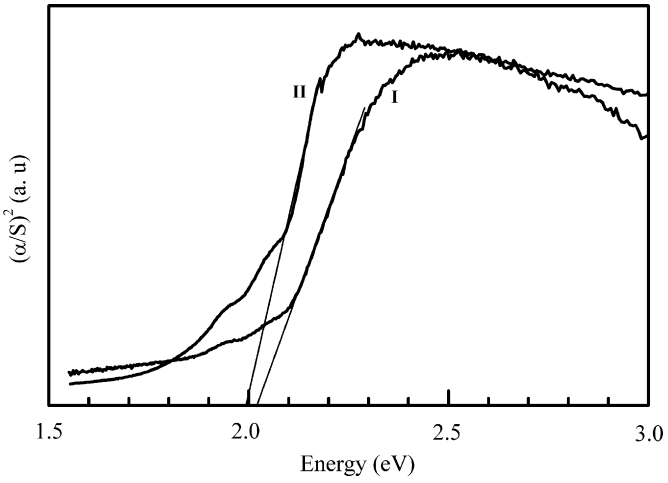


Fig. 7. Diffuse reflectance spectra for compounds **I** and **II**.

chalcogenides with main group, rare earth and alkali metal constituents; however, a similar relationship of ordered (superstructure) and disordered cations derived from the pure antifluorite-type structure is well documented in lithium-containing ternary intermetallics, for example, $Li_7NbP_4$ and $Li_7NbN_4$ (superstructure) [39,40].

### 3.2. Spectroscopic analysis

The Raman spectra of **I** and **II** are very similar (Fig. 6) as expected from their structural similarity especially with respect to the environment of Ge atoms. The Raman spectrum of $GeSe_2$, where 4 Se atoms are in the local environment of Ge forming a tetrahedron, was analyzed by Popovic [41]. In the Raman spectrum of $GeSe_2$, the most intense peak at 212 $cm^{-1}$ was assigned to the symmetric bond stretching $\upsilon_1$ ($A_1$) mode, while higher frequency (251−329 $cm^{-1}$) and lower frequency (50−150 $cm^{-1}$) peaks are due to the asymmetric bond stretching ($E$) and bond bending ($F$) vibration modes of $GeSe_4$ tetrahedron. **I** and **II** also contain the $GeSe_4$ building unit, so employing the same argument as Popovic, the strong peaks at 199 and 201 $cm^{-1}$, for **I** and **II**, respectively, can be assigned to the primary symmetric stretching ($A_1$ mode, $\upsilon_1$) of $GeSe_4$ tetrahedra. Besides the signature of the strong $A_1$ mode, the spectra also consist of several weak peaks in the lower (123.8, 147 $cm^{-1}$) and higher (267.6, 289 $cm^{-1}$) energy regions, which can be tentatively assigned to the bending ($F$) and asymmetric stretching modes ($E$) of $GeSe_4$ tetrahedra.

The analysis of the UV–vis diffuse reflectance spectra of **I** and **II** employing the Kubelka–Munk function [37] indicate that they are semiconducting and the optical band gap of the two compounds are nearly identical at 2.03 and 2 eV, respectively, for **I** and **II** (Fig. 7). The band gaps of the materials are consistent with the observed red color of the crystals and slightly lower than the related Eu-containing cubic phase, $Ag_{0.5}Eu_{1.75}GeS_4$ [26], which has a band gap of 2.14 eV.

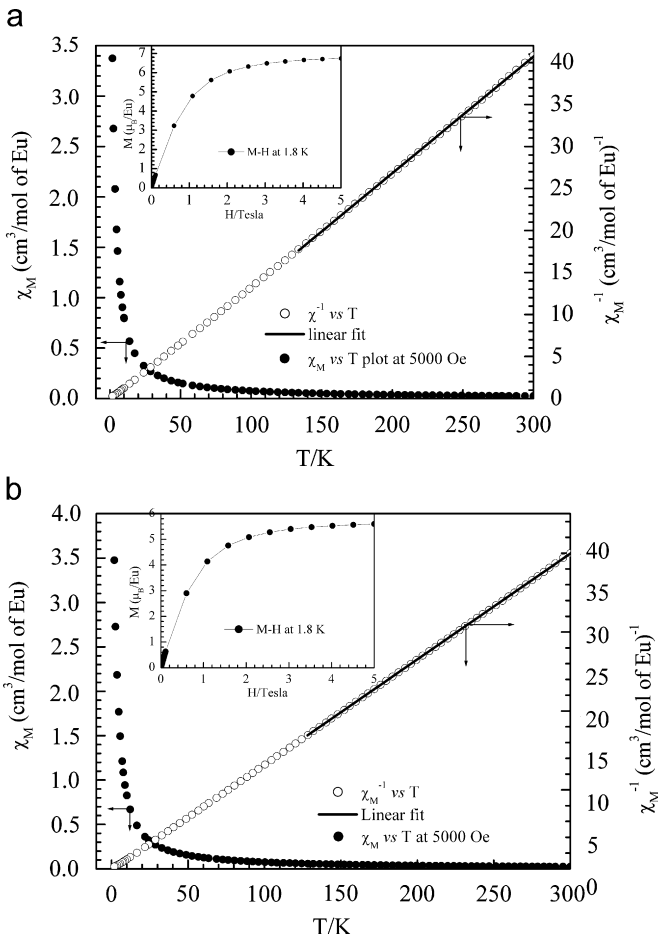


Fig. 8. Plots of the magnetic susceptibility ($\chi$) and inverse susceptibility ($\chi^{-1}$) of **I**, (a), and **II**, (b), as a function of temperature. The thick lines in the high temperature region of the $\chi^{-1}$ ($T$) plot indicate the linear fitting of the data points. The insets show the isothermal magnetization at 1.8 K.

### 3.3. Magnetic measurements

The plot of the temperature dependence of the magnetic susceptibility ($\chi$) and inverse-susceptibility ($\chi^{-1}$) of **I** and **II** in the range 2−300 K are given in Fig. 8(a) and (b), respectively. The asymptotic nature of the $\chi(T)$ plots at 5000 Oe (1 T = 10 000 Oe) under field-cooled and zero-field cooled (FC and ZFC) conditions indicate paramagnetic behavior of the compounds and no magnetic transitions are observed under these conditions (at an applied field of 0.5 T). The absence of any transition in **I** is also established by the FC and ZFC $\chi(T)$ measurements under low applied field (10 Oe), which are again asymptotic. The plots of $\chi^{-1}(T)$ at 5000 Oe show linear behavior above 10 K and the data in the range 150−300 K could be fitted to the Curie-Weiss law, $\chi = C/(T-\theta)$, thus yielding the values of the effective moment ($\mu_{\text{eff}}$) of 7.6 and 7.73 $\mu_B$, and the paramagnetic Curie temperature ($\theta_p$) as +5.15 and +1.86 K for **I** and **II**, respectively. The effective paramagnetic moments are close to the theoretical magnetic moment of 7.93 $\mu_B$ expected for Eu in oxidation state +2 with seven *f*-electrons and the positive sign and small magnitude of $\theta_p$ indicate a very weak ferromagnetic correlation in the paramagnetic region. However, when the susceptibility data for **II** was collected under a low applied field (10 Oe) in both FC and ZFC conditions, there appeared to be a transition at 4.4 K. There is a very marginal divergence of the FC and ZFC $\chi(T)$ plot after the transition point at 10 Oe applied field (Fig. 9). The AC susceptibility measurement also indicated the presence of a transition but did not show any frequency dependence of the transition temperature. However, the kink at 4.4 K in the $\chi(T)$ plot was attenuated slightly above 100 Oe and completely disappeared for fields above 1000 Oe, indicating that this could be metamagnetic transition. However, we could not notice any discontinuity in the *M*–*H* curve when closely spaced data were collected. So the exact nature of the transition is not clear at this point. It could be due to a small amount of the paramagnetic impurity. To validate such possibility, a larger single crystal needs to be grown so that magnetic measurements can be done on a single crystal. The isothermal magnetization (*M*) measured at 1.8 K for both the compounds does not seem to saturate even at 5 T, and the value of saturation moments at 5 T are about 6.74 $\mu_B$/Eu (see inset of Fig. 8a) and 5.6 $\mu_B$/Eu (see inset of Fig. 8b) for **I** and **II**, respectively. The saturation moment of 6.74 $\mu_B$/Eu in case of **I** is close to the theoretical saturation moment of 7 $\mu_B$/Eu, indicating that at low temperature and high field (5 T) an almost parallel spin of the electrons of Eu in $Na_2EuGeSe_4$ can be reached. The paramagnetic moment and magnetization behavior of **I** and **II** are similar to several $Eu^{2+}$ containing main group chalcogenides, $Eu_2GeSe_4$, $Eu_2Ge_2Se_5$ [42], $Eu_2GeS_4$ [43] and $Eu_2SnS_4$ [44].

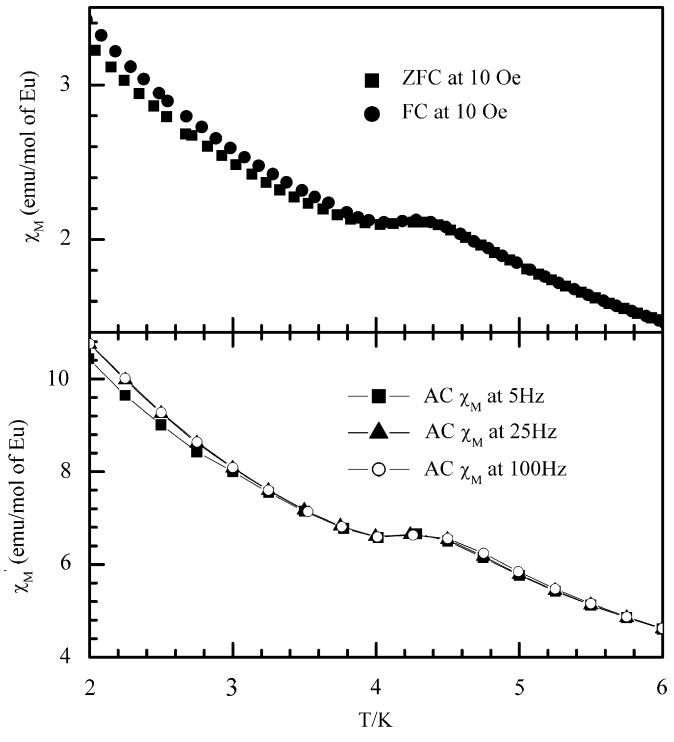


Fig. 9. The FC and ZFC DC susceptibility data of **II** at 10 Oe applied field (top plot). The AC susceptibility data are plotted at various frequencies (bottom plot).

## Acknowledgments

The authors wish to acknowledge financial support provided by the National Science Foundation, NSF-DMR-0343412. The authors also thank Dr. Thomas Schleid and his group, University of Stuttgart, for performing numerical absorption correction on our data sets.

## References

[1] P. Wu, J.A. Ibers, J. Alloys Compds. 229 (1995) 206.
[2] M.R. Davolos, A. Garcia, C. Fouassier, P. Hagenmuller, J. Solid State Chem. 83 (1989) 316 and references cited therein.
[3] M. Tampier, D. Johrendt, J. Solid State Chem. 158 (2001) 343.
[4] J.A. Cody, M.F. Mansuetto, S. Chien, J.A. Ibers, Mater. Sci. Forum 35 (1994) 152.
[5] M.G. Kanatzidis, A.C. Sutorik, Prog. Inorg. Chem. 43 (1995) 151.
[6] I. Hartenbach, Th. Schleid, Z. Anorg. Allg. Chem. 629 (2003) 394.
[7] B.R. Martin, P.K. Dorhout, Inorg. Chem. 43 (2004) 385.
[8] A. Choudhury, P.K. Dorhout, Inorg. Chem. 45 (2006) 5245.
[9] P. Wu, J.A. Ibers, J. Solid State Chem. 107 (1993) 347.
[10] C.K. Bucher, S.-J. Hwu, Inorg. Chem. 33 (1994) 5831.
[11] G. Gauthier, F. Guillen, S. Jobic, P. Deniard, P. Macaudière, C. Fouassier, R. Brec, Acad. Sci. Paris Ser. II 2 (1999) 611.
[12] I. Hartenbach, Th. Schleid, Z. Anorg. Allg. Chem. 628 (2002) 1327.
[13] C.R. Evenson IV., P.K. Dorhout, Inorg. Chem. 40 (2001) 2409.
[14] B.C. Chan, P.K. Dorhout, Z. Kristallogr. 220 (2005) 7.
[15] A.K. Gray, J.M. Knaust, B.C. Chan, L.A. Polyakova, P.K. Dorhout, Z. Kristallogr. 220 (2005) 293.
[16] I. Hartenbach, Th. Schleid, Z. Anorg. Allg. Chem. 631 (2005) 1365.
[17] I. Hartenbach, Th. Schleid, J. Alloys Compds. 418 (2006) 95.
[18] B.R. Martin, L.A. Polyakova, P.K. Dorhout, J. Alloys Compds. 408–412 (2006) 490.
[19] H.A. Graf, H. Schaefer, Z. Anorg. Allg. Chem. 425 (1976) 67.
[20] B. Eisenmann, R. Zagler, Z. Naturforsch. B 44 (1989) 249–256.

[21] C. Crevecoeur, Acta Crystallogr. 17 (1964) 757.
[22] J. Li, H.-Y. Guo, D.M. Proserpio, A. Sironi, J. Solid State Chem. 117 (1995) 247.
[23] C.L. Teske, Z. Anorg. Allg. Chem. 522 (1985) 122.
[24] J.A. Aitken, G.A. Marking, M. Evain, L. Iordanidis, M.G. Kanatzidis, J. Solid State Chem. 153 (2000) 158.
[25] K.M. Poduska, L. Cario, F.J. DiSalvo, K. Min, P.S. Halasyamani, J. Alloys Compds. 335 (2002) 105.
[26] R.G. Iyer, J.A. Aitken, M.G. Kanatzidis, Solid State Sci. 6 (2004) 451.
[27] L.D. Gulay, M.R. Huch, M. Wołcyrz, I.D. Olekseyuk, J. Alloys Compds. 402 (2005) 115.
[28] J.A. Aitken, P. Larson, S.D. Mahanti, M.G. Kanatzidis, Chem. Mater. 13 (2001) 4714.
[29] J.-H. Liao, M.G. Kanatzidis, Inorg. Chem. 31 (1992) 431.
[30] B. Eisenmann, J. Hansa, H. Schaefer, Mater. Res. Bull. 20 (1985) 1339.
[31] B. Eisenmann, J. Hansa, H. Schaefer, Z. Naturforsch. B 40 (1985) 450.
[32] G. Dittmar, H. Schaefer, Acta Crystallogr. B 32 (1976) 2726.
[33] SAINT, Data processing software for the SMART system, Bruker Analytical X-ray Instruments, Inc., Madison, WI, 1995.
[34] W. Herrendorf, H. Bärnighausen, HABITUS; Program for the optimization of the crystal shape for numerical absorption Correction in X-SHAPE (version 1.06, Fa. Stoe, Darmstadt 1999); Karlsruhe, Gießen, Germany 1993, 1996.
[35] G.M. Sheldrick, *SHELXS-97*, Program for X-ray Crystal Structure Solution, University of Göttingen, Germany, 1997.
[36] G.M. Sheldrick, *SHELXL-97*, Program for X-ray Crystal Structure Refinement, University of Göttingen, Germany, 1997.
[37] W.W. Wendlandt, H.G. Hecht, Reflectance Spectroscopy, Interscience Publishers, New York, 1966.
[38] A.R. West, Solid State Chemistry and its Applications, Wiley, New York, 1987.
[39] L. Monconduit, M. Tillard-Charbonnel, C. Belin, J. Solid State Chem. 156 (2001) 37.
[40] D.A. Vennos, F.J. DiSalvo, Acta Crystallogr. C 48 (1992) 113.
[41] Z.V. Popović, Fizika 15 (1983) 11.
[42] M. Tampier, D. Johrendt, R. Pöttgen, G. Kotzyba, C. Rosenhahn, B.D. Mosel, Z. Naturforsch. B 57 (2002) 133.
[43] M. Tampier, D. Johrendt, R. Pöttgen, G. Kotzyba, H. Trill, B.D. Mosel, Z. Anorg. Allg. Chem. 628 (2002) 1243.
[44] R. Pocha, M. Tampier, R.-D. Hoffmann, B.D. Mosel, R. Pöttgen, D. Johrendt, Z. Anorg. Allg. Chem. 629 (2003) 1379.